Ultrasonics - Sonochemistry 44 (2018) 53–63

Contents lists available at ScienceDirect

Ultrasonics - Sonochemistry

journal homepage: www.elsevier.com/locate/ultson

Using ultrasonic (US)-initiated template copolymerization for preparation of an enhanced cationic polyacrylamide (CPAM) and its application in sludge dewatering

Li Feng[a,b], Shuang Liu[a,b,*], Huaili Zheng[a,b,*], Jianjun Liang[b], Yongjun Sun[c], Shixin Zhang[b], Xin Chen[b]

[a] State Key Laboratory of Coal Mine Disaster Dynamics and Control, Chongqing University, Chongqing 400044, China
[b] Key Laboratory of the Three Gorges Reservoir Region's Eco-Environment, Ministry of Education, Chongqing University, Chongqing 400045, China
[c] College of Urban Construction, Nanjing Tech University, Nanjing 211800, China

ARTICLE INFO

Keywords:
Microblock structure
Ultrasonic initiation
Template polymerization
Sludge dewatering
Cationic polyacrylamide
Flocculation

ABSTRACT

In this study, the ultrasonic (US)-initiated template copolymerization was employed to synthesize a novel cationic polyacrylamide (CPAM) characterized by a microblock structure using dimethyldiallylammonium chloride (DMDAAC) and acrylamide (AM) as monomers, and sodium polyacrylate (NaPAA) as template. The polymers structure property was analyzed by Fourier transform infrared spectroscopy (FT-IR), ^{1}H nuclear magnetic resonance spectroscopy (^{1}H NMR) and thermogravimetric analysis (TGA). The results showed that a novel cationic microblock structure was successfully synthesized in the template copolymer of DMDAAC and AM (TPADM). Meanwhile, the analysis result of association constant (M_K) provided powerful support for a I Zip-up (ZIP) template polymerization mechanism and the formation of the microblock structure. The factors affecting the polymerization were investigated, including ultrasonic power, ultrasonic time, monomer concentration, initiator concentration, m_{AM}:m_{DMDAAC} and n_{NaPAA}:n_{DMDAAC}. The sludge dewatering performance of the polymers was evaluated in terms of specific resistance to filtration (SRF), filter cake moisture content (FCMC), floc size (d_{50}) and fractal dimension (D_f). Flocculation mechanism was also analyzed and discussed. The sludge dewatering results revealed that the polymer with the novel microblock structure showed a more excellent flocculation performance than those with randomly distributed cationic units. A desirable flocculation performance with a SRF of 4.5×10^{12} m kg^{-1}, FCMC of 73.1%, d_{50} of 439.156 μm and D_f of 1.490 were obtained at pH of 7.0, dosage of 40 mg L^{-1} and the molecular weight of 5.0×10^6 Da. The cationic microblock extremely enhanced the polymer charge neutralization and bridging ability, thus obtaining the excellent sludge dewatering performance.

1. Introduction

Due to the accelerating rate of urbanization, the increasing worldwide establishment and operation of sewage treatment plants, a large number of excessive activated sludge has been produced in the process of biological treatment processes [1,2]. In China, about 1.506×10^9 tons of activated sludge is generated every year, and which has resulted in serious problems in transportation, treatment and disposal [3]. It was well documented that active sludge was highly compressible but difficult to dewatering mainly because the active sludge had high water content (> 97%), presence of organic components (bacterial cells and extracellular polymeric substances (EPS)), colloidal and supracolloidal speciality and biological gel structure properties [4–6]. Thus, how to enhance the sludge dewatering performance and reduce the moisture content of sludge filter cake has become more urgent and significant.

Chemical conditioning by the cationic polyacrylamides (CPAMs) has been extensively used in the process of sludge dewatering owing to their advantages such as less dosage, higher efficiency, facile operation and affordable price [7,8]. The active sludge colloids were neutralized and destabilized through charge neutralization and the destabilized sludge colloids subsequently agglomerated by CPAMs to form large and dense flocs under the effect of bridging, thereby reducing the sludge moisture content and volume [9,10]. Despite the fact that the various types of commercial CPAMs have been developed and used successfully in sludge dewatering, there is still a need to improve their efficiency and develop new types of polymers for the enhancement of sludge dewatering performance. Disappointedly, a significant drawback in the

* Corresponding authors at: State Key Laboratory of Coal Mine Disaster Dynamics and Control, Chongqing University, Chongqing 400044, China.
E-mail addresses: liushuang_cqu@163.com (S. Liu), hlz6512@163.com (H. Zheng).

https://doi.org/10.1016/j.ultsonch.2018.02.017
Received 23 October 2017; Received in revised form 6 February 2018; Accepted 6 February 2018
Available online 07 February 2018
1350-4177/ © 2018 Elsevier B.V. All rights reserved.

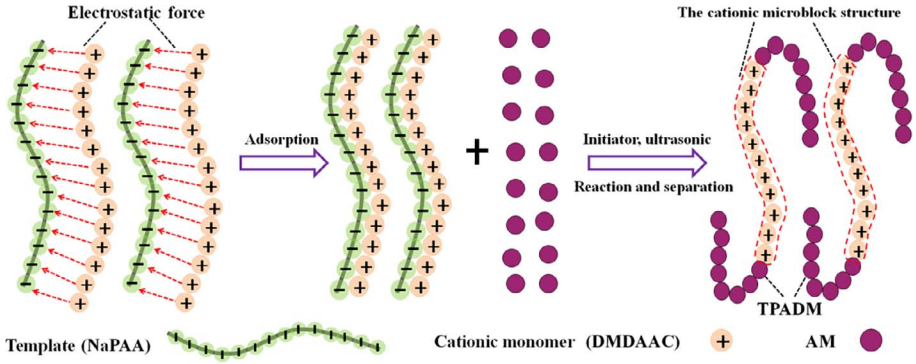


Fig. 1. The basic principle for the template polymerization technology.

aforementioned CPAMs exists: the cationic units distributes randomly in the CPAMs molecular chain, which will waste a part of cationic monomers and weaken the charge neutralization ability. As a result, the further improvement and enhancement of sludge dewatering ability is limited by the deficiency of disordered and random cationic units distribution in the polymer chain.

Fortunately, template polymerization technology provided a new way for the research of CPAMs, which could be used to prepare the flocculant with a microblock structure [11]. Its basic principle is shown in Fig. 1. Just as that of the gene translation process, the cationic monomers are adsorbed and arranged on the molecular chain of the anionic template NaPAA under the electrostatic force to form the precursor of the microblock structure. Once the copolymerization reaction is initiated by the initiator, the pre-adsorbed cationic monomer will be homopolymerized to form a cationic microblock structure. When the template is separated, the novel cationic microblock structure in the copolymer is successfully obtained. Because of the cationic microblock structure in polymer chain, the positive charge density and the utilization efficiency of cationic monomers are greatly improved, and thereby the ability of charge neutralization is greatly strengthened. Moreover, ultrasonic initiation has gained considerable attention and interest depending on their faster polymerization rate, lower reaction temperature, higher monomer conversion and smaller amount of initiator than other initiation systems [12–14]. Therefore, it is inspired to employ the ultrasonic (US)-initiated polymerization technique for preparing the cationic microblock structure in the polymer chain for the application in enhancing sludge dewatering. To the best of our knowledge, the less toxic dimethyldiallylammonium chloride (DMDAAC) and acrylamide (AM) are the most commonly used monomers to synthesize the CPAM [15,16], and hence it is more meaningful and constructive to design a polymer with a novel microblock structure through US-initiated template copolymerization by using AM and DADAAC.

In this study, the primary objectives were to: (1) prepare the flocculant with the cationic microblock structure through US-initiated template copolymerization using AM and DADAAC as monomers, and NaPAA as template. (2) investigate the polymer characters such as structure and thermal decomposition properties by using Fourier transform-infrared spectroscopy (FTIR), ^{1}H nuclear magnetic resonance (^{1}H NMR), and thermogravimetric analysis (TGA). (3) Study the effect of synthesis conditions (ultrasonic power, ultrasonic time, monomer concentration, initiator concentration, m_{AM}:m_{DMDAAC} and n_{NaPAA}:n_{DMDAAC}) on the copolymerization. (4) Discuss the template copolymerization mechanism through the association constant (M_K). (5) Evaluate the impact of the microblock structure on sludge dewatering performance in terms of specific resistance to filtration (SRF), cake moisture content (FCMC), floc size and fractal dimension. And (6) discuss and summarize the possible flocculation mechanism.

2. Materials and methods

2.1. Materials

The details of the materials used in this study were as follows: Acrylamide (AM) (industrial grade; Chongqing Lanjie Tap Water Company, Chongqing, China), Dimethyldiallylammonium chloride (DMDAAC) (65 wt% in water and industrial grade; Jinan Yifan Chemical Co., Ltd. Jinan, China), Template sodium polyacrylate (NaPAA) (industrial grade; Molecular weight: 4200, Shandong Xintai Water Treatment, Xintai, China), Initiator 2,2′-azobis [2-(2-imidazolin-2-yl) propane] dihydrochloride (VA-044) (analytical reagent grade; Ruihong Biological Technology, Shanghai, China), Absolute ethyl alcohol and acetone (analytical reagent grade) were obtained from Chongqing Chuandong Chemical Industry Co., Ltd (Chongqing, China). All aqueous and standard solutions were prepared with deionized water. Commercial flocculants CCPAM (copolymerization of AM and methacryloxyethyl trimethyl ammonium chloride (DMC)) and CCPAD (copolymerization of AM and acryloyloxyethyl trimethyl ammonium chloride (DAC)) were the gift of Chongqing Lanjie Tap Water Company, (Chongqing, China).

2.2. Preparation of copolymers

The synthesis reaction of the polymer was initiated by ultrasonic wave generated by an ultrasonic equipment (Sonics Vibra-cell, VCX 500; Power: 0–500 W, Frequency: 20 kHz; Shenzhen koguang ultrasonic equipment co. LTD, Shenzhen, China). Besides, the generator with a sonic wave probe (tip diameter: 13 mm, length: 136 mm) is of horn type. The ultrasonic irradiation is an indirect irradiation, and the distance between ultrasonic generator and reaction solution is 5 cm. Meanwhile, the low temperature cooling circulating water bath system is used to regulate the temperature. The steps of the US-initiated template copolymerization for TPADM were shown as follows. A certain amount of AM, DMDAAC, NaPAA (n_{NaPAA}:n_{DMDAAC} = 1:1) and deionized water was added into a 100 mL quartz jar, where the pH of the reaction solution (41.8 mL) was adjusted to 4.5 by 0.1 mol L^{-1} HCl and NaOH. The reaction vessel was purged with nitrogen with a flow rate of 40 mL min^{-1} for 30 min to remove oxygen completely after adding a given dose of initiator VA-044 to the mixture. Then, the quartz jar was sealed immediately and exposed under the ultrasonic radiation for 5–35 min at 35–45 °C to initiate the reaction. Finally, the formed copolymer was purified by acetone and ethanol and dried in a vacuum oven at 90 °C until a constant weight was obtained. The preparation of CPADM was similar to that of TPADM except that no template was used and the proposed reaction routes for TPADM and CPADM were illustrated in Fig. 2.

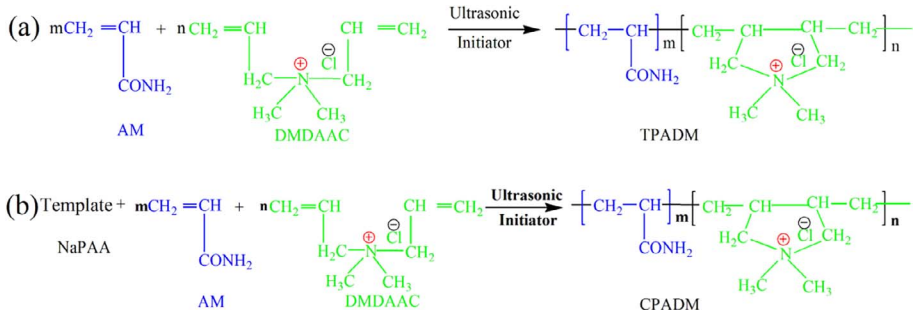


Fig. 2. The proposed reaction routes for (a) TPADM and (b) CPADM.

2.3. Characteristics of copolymers

Based on the previous research, the gravimetric and one point methods were used to determine the total monomer conversion and the intrinsic viscosities of polymers (η), respectively [17,18]. The polymer molecular weight (MW) used to assess the absorption and bridging ability was related to the intrinsic viscosity (η) and it could be calculated according to the following Eq. (1).

$$M_r = 802[\eta]^{1.25} \quad (1)$$

where $[\eta]$ is the intrinsic viscosity (mL/g) and M_r is the molecular weight of the polymer. Besides, the positive charge density of the polymers used to evaluate the charge neutralization ability was determined by titration method [19]. Poly (vinyl sulfate) potassium salt (PVSK) and toluidine blue O (TBO) were used as titrant and indicator, respectively.

FT-IR analyses of the polymers were conducted on a 550 Series II infrared spectrometer (Mettler Toledo Instruments Co., Ltd., Switzerland). ^{1}H NMR analyses were performed on an Avance 500 nuclear magnetic resonance spectrometer (Bruker Company, Ettlingen, Germany) using deuterium oxide (D_2O) as solvent. Thermogravimetric analysis (TGA) was recorded on a DTG-60H synchronal thermal analyzer (Shimadzu, Kyoto, Japan) at a heating rate of 10 °C·min^{-1}, nitrogen flow of 20 mL·min^{-1}, and temperature range of 20–600 °C.

2.4. Determination of K_M

In order to investigate the possibility of forming microblock structure and the template polymerization mechanism involved in the US-initiated template copolymerization process, the association constant (K_M) between DMDAAC and NaPAA was examined [20]. Dialyses and conductance titration method was used to obtain the K_M value. A certain amount of NaPAA was added into a dialysis bag (Intercepted, M_WCO 4000, MD 25, USA) and soaked in the deionized water for a 24 h dialysis. Therefore, the NaPAA intercepted by the dialyses would become more similar because the NaPAA with a molecular weight less than 4000 was dialyzed away. The intercepted NaPAA was precipitated by using acetone and dried in a vacuum oven at 90 °C for 24 h, and then the dried NaPAA (0.01 mol) and DMDAAC (0.01 mol) were added into 100 mL deionized water to form a mixed aqueous solution. Subsequently, the pH of the above NaPAA and DMDAAC mixed aqueous solution was adjusted to a set value of 4.5 and kept for 24 h at room temperature to reach an adsorption-desorption balance. The K_M was determined through the following Eq. (2):

$$K_M = \frac{[\text{NaPAA}{*}{*}{*}{*}\text{DMDAAC}]}{[\text{NaPAA}]_f\,[\text{DMDAAC}]_f} \quad (2)$$

In Eq. (2), $[NaPAA]_f$ and $[DMDAAC]_f$ were the free concentrations at adsorption-desorption balance. $[NaPAA_{****}DMDAAC]$ was the concentration of the association of NaPAA and DMDAAC and it could be calculated through the following Eq. (3):

$$[NaPAA{*}{*}{*}{*}DMAAAC] = [NaPAA]_0([DMDAAC]_0) - [NaPAA]_f([DMDAAC]_f \quad (3)$$

where $[NaPAA]_0$ and $[DMDAAC]_0$ were the initial concentration of NaPAA and DMDAAC. $[NaPAA]_f$ and $[DMDAAC]_f$ were the same as those in Eq. (2), and the value of which could be calculated by the conductometric titration method.

2.5. Dewatering experiment

In sludge dewatering experiment, the flocculants used for the dewatering tests were shown in Table 1 and the flocculants had the same intrinsic viscosity and cationic degree for comparison analyses. Raw sludge was sampled from sludge thickener of Dadukou Drainage Co., Ltd. and it came from a cyclic-activated sludge system. The characteristics of the used flocculants are listed in Table 2. The sludge dewatering experiment was performed on a program-controlled Jar-test apparatus (ZR4-6, Zhongrun Water Industry Technology Development Co. Ltd., China). About 250 mL sludge was transferred into a 500 mL glass beaker, and the initial pH of the sludge was adjusted to the set value by HCl (0.1 mol L^{-1}) and NaOH (0.1 mol L^{-1}). A certain dosage of flocculant was added to the glass beaker with a rapid stirring at 200 rpm for 30 s to achieve complete mixing of the flocculant and sludge, then a slow stirring at 50 rpm for 10 min to enhance the flocs growth, and no stirring for 10 min for the flocs settling [21]. FCMC, SRF, floc size and fractal dimension (D_f) were used to evaluate the flocculation ability of the polymers, and the detail analytical methods of FCMC, SRF and D_f were described in Supporting Text S1. The zeta potential of supernatant and flocs size were conducted on a Zetasizer Nano ZS90 (Malvern Instruments Ltd., Malvern, UK) and a laser diffraction instrument (Mastersizer 2000, Malvern, U.K.), respectively. Each test was repeated in triplicate and the average of three runs was recognized as the final result.

Table 1
The details of flocculants used for the characterization and jar tests.

Flocculants[a]	Cationic monomer molar content (%)	Molecular weight (1×10^6Da)	Conversion rate (%)	Synthetic method
TPADM	30.0	4.99	99.7	USTP
CPADM	30.0	5.01	99.6	N-USTP
CCPAD	30.0	5.00	99.8	/
CCPAM	30.0	5.00	99.8	/
PAM	/	5.00	99.8	N-USTP

[a] TPADM: template copolymer of DMDAAC and AM by US-initiated template copolymerization (USTP); CPADM: copolymer of DMDAAC and AM by non US-initiated template copolymerization (N-USTP); PAM: homopolymer of AM by N-USTP; CCPAD: commercial copolymer of DAC and AM; CCPAM: commercial copolymer of DMC and AM.

Table 2
Characteristics of sludge.

Indicator	pH	Mass density (g/ml)	Zeta potential (mV)	Moisture content (wt%)	VSS/TSS
Value	6.93 ± 0.1	0.978	−24.9 ± 0.1	98.9 ± 0.15	0.73

3. Results and discussion

3.1. Optimizing synthesis conditions

3.1.1. Effect of ultrasonic power on copolymerization

As ultrasound waves pass through liquid media, cavities generated by oscillating acoustic pressures will grow in size and ultimately implode, and thereby more energy will be released. This released energy will promote the molecular collision and accelerate the initiator division for more free radical, and thus initiating the monomers copolymerization [22]. As shown in Fig. 3(a), the effect of ultrasonic power on copolymerization was investigated at ultrasonic time of 20 min, monomer concentration of 30 wt%, initiator concentration of 0.06 wt‰, m_{AM}:m_{DMDAAC} = 3:1 and n_{NaPAA}:n_{DMDAAC} = 1:1. It was found that the ultrasonic wave with the 150 W was more suitable for the copolymerization, whereas the higher or lower ultrasonic power than 150 W was unfavorable for the copolymerization. At lower ultrasonic power, the initiation energy was not strong to generate enough free radical and the monomers collision was also not thorough. Consequently, the copolymerization efficiency declined and the molecular weight and conversion decreased. By contrast, the higher ultrasonic power would generate enough free radical within short time and the violent collision of monomers, and the increment of recombination would cause a decrement of the initiator efficiency. Consequently, an evident decrement of molecular weight and a slight reduce of the conversion were observed for the polymer. Besides, more strong shear force caused by the cavities swell and collapse would destroy and cut off the formed polymer chain, thus leading to a low molecular weight [23]. Based on the above analyses, a relatively higher powerful ultrasonic power (150 W) was necessary for a high-efficiency copolymerization.

3.1.2. Effect of ultrasonic time on copolymerization

Comparing with thermal initiator methods, US-initiated polymerization is demonstrated to be a more efficient and energy saving methods. The effect of ultrasonic time on polymerization was evaluated, where ultrasonic power, monomer concentration, initiator concentration, m_{AM}:m_{DMDAAC} and n_{NaPAA}:n_{DMDAAC} = 1:1 were deemed to be 150 W, 30 wt%, 0.06 wt‰, 3:1 and 1:1, respectively. In Fig. 3(b), the molecular weight and conversion increased fast with the radiation time increase from 5 min to 15 min. Moreover, when the radiation time exceeded 20 min, no increase of the molecular weight and conversion intrinsic was observed. The initiator could generally be decomposed by ultrasonic radiation and generate free radicals. The sufficient constant radiation of 20 min could generate enough free radicals to accelerate the molecular bond breakage and aggrandize graft sites, thereby resulting in the rapid growth of the molecular weight and conversion [24]. However, when radiation time was over than 20 min, free radicals

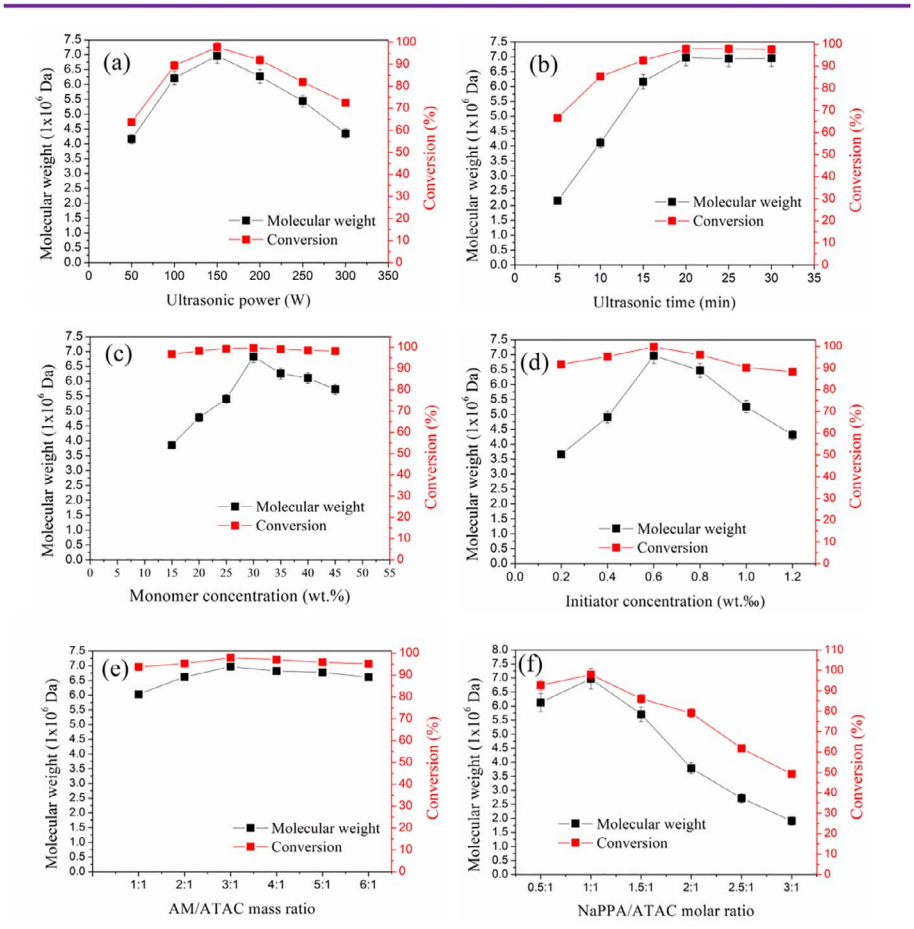


Fig. 3. Effect of (a) ultrasonic power, (b) ultrasonic time (c) monomer concentration (d) initiator concentration, (e) AM/DMDAAC mass ratio and (f) NaPPA/DMDAAC molar ratio on polymerization.

no longer formed due to the complete exhaustion of initiator and molecular bond in the first reaction step within 20 min. As a result, the continue radiation time of more than 20 min had no impact to the molecular weight and conversion. Therefore, 20 min was chosen as the optimal ultrasonic radiation time in this study.

3.1.3. Effect of monomer concentration on copolymerization

Fig. 3(c) displayed the effect of monomer concentration on molecular weight and conversion, and the other factors were constant. When the monomer concentration increased to 30 wt%, the chance of monomers collision and the amount of free radicals reached the peak value, thus accelerating the rate of chain propagation and further increased the molecular weight. In this condition, a slight increase for the conversion was also observed. However, with the further increased of monomer concentration, the molecular weight and conversion exhibited a slightly decreasing trend. Chain transfer and chain termination always occurred at excessive monomer concentration, thereby resulting in a decrease of molecular weight [7,25]. It was obvious that the conversion is almost constant and the decrease of conversion is marginal at high monomer concentration. Consequently, the favorable value of monomer concentration used in this study was 30 wt%.

3.1.4. Effect of initiator dosage on copolymerization

The initiator is the active center of the free radical polymerization reaction, and which is an important factor in the US-initiated copolymerization. Therefore, the effect of initiator dosage on molecular weight and conversion was investigated, while the remain factors were kept constant. As shown in Fig. 3(d), the result illustrated that the molecular weight aggrandized as the initiator dosage increased from 0.01 wt‰ to 0.06 wt‰ at the early stage of the reaction, but declined rapidly with the further increase of initiator concentration. Meanwhile, a first increasing and then decreasing trend for the conversion was also observed. However, compared with the vibration of molecular weight, that of the conversion was slight and almost constant at high monomer concentration. Few primary free radicals generated at a low initiator dosage were surrounded by a large number of solvent molecules, called as the “cage effect”, which inhibited the formation of monomeric free radicals and further chain growth [8,26]. A relatively higher initiator dosage from 0.04 wt‰ to 0.06 wt‰ was needed for the improvement of molecular weight and conversion. On the contrary, the higher initiator dosage would speed up chain transfer and chain termination, thereby leading to the decrease of molecular weight and conversion. In addition, the crosslinking and implosion caused by the excessive initiator was also adverse for the increase of molecular weight and conversion. Thus, the optimal monomer concentration was adopted as 0.06 wt‰ in this study.

3.1.5. Effect of AM/DMDAAC mass ratio on polymerization

Due to the reactivity ratio differences between AM and DMDAAC in copolymerization, the m_{AM}:m_{DMDAAC} may have impact on the copolymerization. Therefore, the effect of monomer mass ratio on the copolymer molecular weight and conversion was researched while the other factors were constant. As shown in Fig. 3(e), it was obvious that both the molecular weight and conversion first increased to the top value and then decreased with the further increase of m_{AM}:m_{DMDAAC}. The maximum value of molecular weight and conversion was obtained at the m_{AM}:m_{DMDAAC} of 3:1. According to the free radicals mechanism of polymerization, the molecular weight and the conversion of the polymer depended on the number of monomeric free radicals in the early stage of reaction [27]. Because AM had a higher reactivity ratio compared with other monomers, the chance of collision between AM and primary free radicals was enhanced due to the higher AM concentration [28]. Therefore, the chain propagation and higher conversion was more likely to happen. However, excessive AM monomer concentration also enhanced chain transfer and resulted in large amounts of heat that could not be released in time, thereby speeding up the polymer chain termination. As a result, a lower molecular weight and conversion was observed. Therefore, a m_{AM}:m_{DMDAAC} of 3:1 was chosen in this experiment.

3.1.6. Effect of NaPPA/DMDAAC molar ratio on polymerization

The template NaPPA plays a crucial role in the template polymerization and it also directly affects the formation of the cationic microblock structure. Therefore, the NaPPA/DMDAAC molar ratio on the molecular weight and conversion was studied. As shown in Fig. 3(f), the molecular weight and conversion changed greatly at different n_{NaPPA}:n_{DMDAAC}, which indicated that the NaPPA had a great influence on the copolymerization. The conversion was initially reached to the maximum value as the n_{NaPPA}:n_{DMDAAC} molar ratio was increased from 1:2 to 1:1, but it decreased fast with further increase of n_{NaPPA}:n_{DMDAAC}. Besides, a reduction of molecular weight was observed when the n_{NaPPA}:n_{DMDAAC} value was more than 1. After adding the template NaPPA to the reaction system, the cationic monomer DMDAAC was adsorbed and distributed directionally along the template molecular chain under the electrostatic forces. The cationic monomers adsorbed on the NaPPA polymer were easily initiated by the free radicals with low hindrance, thereby strengthening the chain propagation and polymer conversion. On the contrary, the higher n_{NaPPA}:n_{DMDAAC} would led to a decrease of the molecular weight and conversion. Because of the NaPPA with the $-COO^-$ group had large steric hindrance, superfluous NaPPA would wrap and swathe the DMDAAC to form a cage effect, which distinctly lowered the chance of free radicals collision and inhibited the reaction [29]. As a consequence, the molecular weight and conversion of the polymer all reduced. In this study, a n_{NaPPA}:n_{DMDAAC} of 1:1 was selected for template copolymerization system.

3.2. The association constant (K_M) and template polymerization mechanism

In this study, the association constant (K_M) between DMDAAC and NaPAA was investigated at n_{NaPPA}:n_{DMDAAC} = 1, and a K_M value of 12.85 was acquired. The higher K_M value was, the larger the proportion of DMDAAC absorbed by NaPAA become. According to the Eq. (2), a K_M value of 12.85 means that more than three quarters of the DMDAAC was pre-absorbed and anchored on the polymer molecular chain of NaPAA to form precursor of microblock structure through the electrostatic force between DMDAAC and NaPAA. The K_M value was crucial for understanding the US-initiated template copolymerization mechanism, and a possible ZIP (I) mechanism was obtain through the analysis of K_M value. The DMDAAC was first absorbed by NaPAA to breed a microblock segment, and then the microblock segment was homopolymerized under the ultrasonic radiation to form the microblock structure. After the separation of the template NaPAA, a copolymer (TPADM) with the cationic microblock structure was successfully prepared. The ZIP (I) template polymerization mechanism was illustrated in Fig. 4, and which was a forceful evidence for the formation of the cationic microblock structure in the copolymer chain of TPADM.

3.3. Characterization of flocculants

3.3.1. FTIR spectral analysis

The FT-IR spectra of PAM, CPADM and TPADM were investigated and the results were shown in Fig. 5. The adsorption peaks at 3442 and 1665 cm^{-1} were assigned to the stretching vibration of $-NH_2$ and C=O groups in AM, respectively [8,30]. The asymmetric stretching vibrations of $-CH_3$ and $-CH_2-$ groups were observed at 2943 and 2843 cm^{-1}, respectively [7,25]. The adsorption peak at 1454 cm^{-1} was derived from the bending vibration of $-CH_2-$ in the $-CH_2-N^+$ group of DMDAAC [15]. The characteristic adsorption peak at 954 cm^{-1} was attributed to the $-CH_3$ bending vibrations in $-N^+(CH_3)_2-$ group of DMDAAC [24]. After the copolymerization of AM and DMDAAC, the adsorption peaks of AM and DMDAAC all emerged in the CPADM and

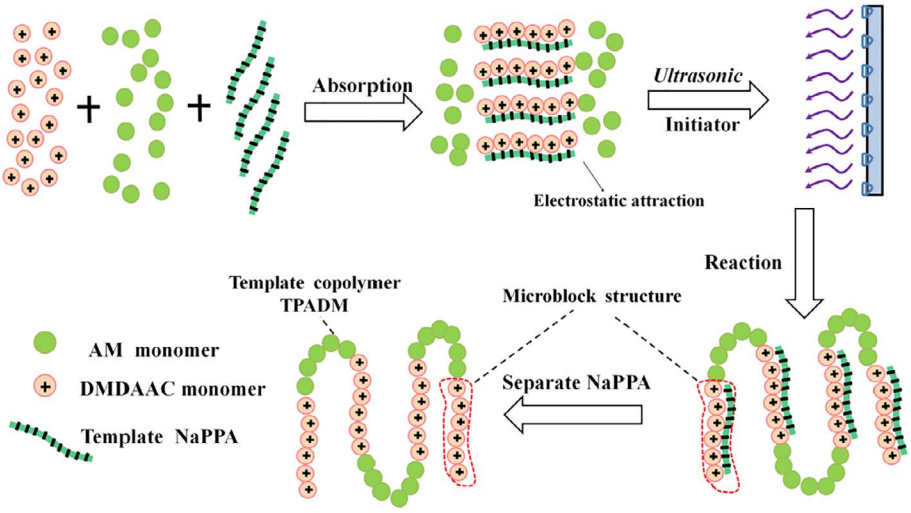


Fig. 4. The possible mechanism for template copolymerization.

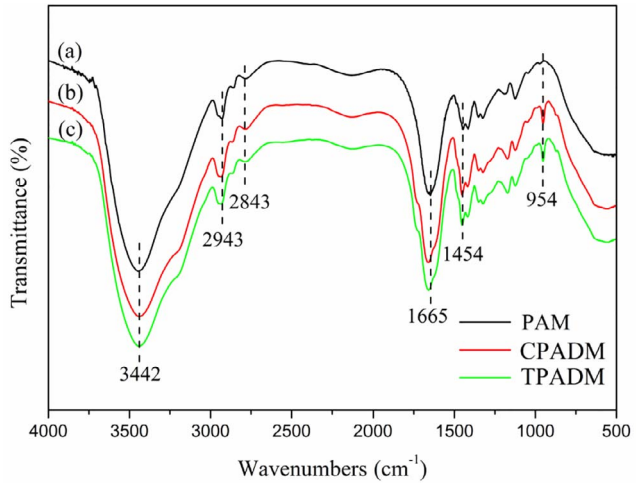


Fig. 5. FT-IR spectra of (a) PAM and (b) CPADM and TPADM.

TPADM, which indicated that CPADM and TPADM were successfully synthesized through the reaction of AM and DMDAAC. Besides, it was found that the adsorption peaks of the CPADM and TPADM were similar except for the difference in the peak area. It means that that the two polymers had the same functional group.

3.3.2. ^1H NMR spectral analysis

Parallel to the FTIR spectrum, the ^1H NMR regarded as an effective method was used to identify the copolymers molecular structure. To investigate the effect of template copolymerization on the polymer microstructure, the ^1H NMR of CPADM, TPADM and PAM were compared and the results were shown in Fig. 6. The absorption peaks at $\delta = 1.66$ ppm and $\delta = 2.23$ ppm were assigned to the protons for $-CH_2-$ (a) and $-CH-$ (b) in PAM, respectively [7,27]. Compared with PAM, a chemical shift occurred for $-CH_2-$ (a) and $-CH-$ (b) groups in CPADM and TPADM, and they were shown at $\delta = 1.71$ ppm and $\delta = 2.28$ ppm, respectively. The main reason for this phenomenon was that the original chemical environment for the homopolymer was vastly destroyed after grafting of DMDAAC monomer, and which resulted in a chemical shift. The characteristic adsorption peaks for the copolymer CPADM and TPADM were all observed at $\delta = 2.77$ ppm for $-CH-$ (c) in DMDAAC, $\delta = 3.72$ ppm for $-(CH_2)_2-N^+$ (d), and $\delta = 3.26$ ppm for $(CH_3)_2-N^+$ (e) [31,32]. The above ^1H NMR spectral analyses indicated that the CPADM and TPADM were successfully synthesized by the copolymerization of AM and DMDAAC, which was in keeping with the FTIR spectral analyses. Moreover, several subtle differences between CPADM and TPADM should not be ignored, which was vital for the formation of anionic microblock structure in TPADM. It was found that seven extra peaks marked with different shape symbols at $\delta = 1.24$ ppm, $\delta = 2.06$ ppm, $\delta = 2.53$ ppm, $\delta = 3.11$ ppm, $\delta = 3.89$ ppm, $\delta = 5.77$ ppm and $\delta = 6.08$ ppm were observed for CPADM, whereas those did not appear for the TPADM. The difference between CPADM and TPADM was related to their stereochemistry properties. The protons of $-CH_2-$ (a), $-CH-$ (c), $-(CH_2)_2-N^+$ (d), and $(CH_3)_2-N^+$ (e) in the microblock structure were identical in principle because of the steric and electrostatic repulsion of the pendant groups, and only one resonance was observed for each group [29,33]. By contrast, the random distribution of cationic monomer in CPADM generated a different chemical environment rather than that of TPADM and the protons became different with the adjacent protons. As a result, two or more individual split protons could be observed for each group. The ^1H NMR spectral analytical results were in accordance with the that of K_M illustrated in Section 3.2, which convincingly indicated the formation of cationic microblock structure in TPADM prepared by US-initiated template copolymerization.

3.3.3. Thermogravimetric analysis

The thermal analysis results of CPADM and TPADM were presented in Fig. 7(a and b). Three steps of the thermal decomposition could be observed for CPADM and TPADM, corresponding to their weight loss. The initial weight loss of 13.8% for CPADM and 9.5% for TPADM occurred in the range of 30–210 °C, which could be contributed to the evaporation of intramolecular and intermolecular moisture in the polymers [34]. The second stage occurred in the range of 210–350 °C with a mass loss of 26.4% for CPADM and 27.1% for TPADM, which was assigned to the imine reaction of the amide group and the thermal decomposition of methyl in the quaternary ammonium groups [16,24]. The third stage occurred beyond 350 °C, and mass loss of 42.9 wt% for CPADM and 44.8% for TPADM were observed. This mass loss portion was caused by the carbonization of the copolymer [8,29]. The above thermal analysis results reveled that both CPADM and TPADM had an inferior thermal stabilities. Moreover, two apparent heat absorption peaks in the second stage appeared at 358.2 and 402.4 °C for TPADM, whereas only a single peak was observed at 372.7 °C for CPADM. The thermal gravimetric curves of the polymers were related to their structure. The copolymers synthesized by US-initiated template copolymerization had two different microblock structures, i.e., DMDAAC and AM microblocks, and these two structures exhibited two different heat absorption peaks. However, the monomer in CPADM distributed randomly rather than orderly and no blocky structure formed, and

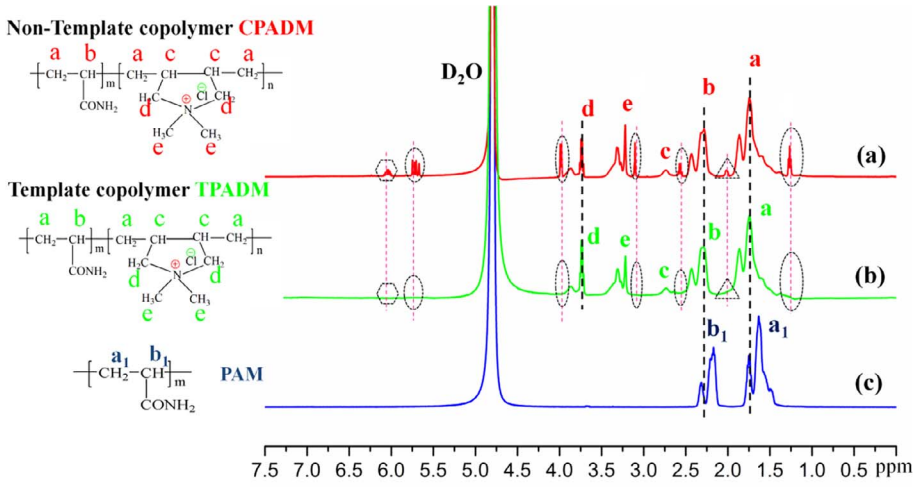


Fig. 6. ^{1}H NMR spectrum of the polymers.

thereby just a single adsorption peak emerged [29,35].

3.4. Dewatering test

3.4.1. Effect of the dosage on sludge dewatering performance

The impact of polymers dosage on FCMC, SRF and zeta potential are investigated and the results were displayed in Fig. 8. The FCMC and SRF for the four flocculants decreased with increasing flocculant dosage before reaching the minimum value at 40 $mg{\cdot}L^{-1}$, and then rapidly increased within the flocculant dosage from 40 to 90 $mg{\cdot}L^{-1}$. When the flocculant dosage was low, the number of the positive charges and the surface active sites of the flocculants were insufficient, and which could not effectively neutralize and adsorb sludge particles, thus resulting in a high FCMC and SRF [28,36]. However, superfluous flocculant dosage would make the colloidal system highly positive charged, which re-stabilized sludge particles through electrostatic repulsion, thereby reducing the dewatering effect [37]. Notably, TPADM showed a superior dewatering performance than the other there in the full dose range, and the minimum values of FCMC and SRF at 40 $mg{\cdot}L^{-1}$ were both in the following order: TPADM (FCMC: 73.1%; SRF: $4.5 \times 10^{12}\ m{\cdot}kg^{-1}$) > CPADM (FCMC: 75.2%; SRF: $5.1 \times 10^{12}\ m{\cdot}kg^{-1}$) > CCPAD (FCMC: 75.7%; SRF: $5.2 \times 10^{12}\ m{\cdot}kg^{-1}$) > CCPAM (FCMC: 76.3%; SRF: $5.6 \times 10^{12}\ m{\cdot}kg^{-1}$). The dewatering ability discrepancy between TPADM and the other three flocculants was related to the cationic microblock in TPADM. As shown in Fig. 8(a), it was found that the zeta potential of the supernatant conditioned with TPADM was much higher than those of CPADM, CCPAD and CCPAM at the same dose. The cationic microblock in TPADM could make full use of cationic units in polymer chain and enhance its charge neutralization effect, and thereby the negative charged colloidal could be neutralized and destabilized by cationic flocculant to form large and compact flocs. Meanwhile, the strong charge repulsion between the polymer chains generated by the cationic microblock was beneficial for the stretch and extension of molecular chain, thus strengthening the bridge effect and further increase the flocculation efficiency [29,37].

3.4.2. Effect of pH on sludge dewatering performance

The pH played an important role in flocculation dewatering because the surface physical and chemical properties of the flocculants was affected greatly by the pH value [38]. Therefore, it was of utmost importance to study the relationship between the dewatering performance and pH value of the sludge at the flocculant dosage of 40 $mg{\cdot}L^{-1}$. As shown in Fig. 9, the FCMC and SRF decreased initially and then increased in the full pH range from 1 to 11, whereas zeta potential displayed a decreased trend. Obviously, the strong acid (pH: 1–4) and alkali (pH: 9–11) conditions was disadvantageous for the sludge dewatering improvement because strong acid/ alkali enhanced the charge intensity on colloidal particles surface and resulted in a strong repulsive force between the sludge particles [39]. As a result, the adsorbed particles would deviate from the polymer chain and the sludge dewatering performance was aggravated. However, the sludge zeta potential increased significantly after adding the cationic flocculant compared with that of origin sludge, and the sludge zeta potential conditioned by TPADM was much higher than that conditioned by CPADM, CCPAD and CCPAM. The above results indicated that charge neutralization played an important role in the flocculation process, and the charge neutralization ability of TPADM could be enhanced greatly by the cationic microblock structure. The cationic microblock generated a strong charge repulsive force and would effectively compress the diffusion layer of negative sludge colloidal particle and reduce its thickness [29,35]. Consequently, the charge repulsion of the negative particles decreased and the sludge dewatering performance become more excellent. In this study, TPADM showed a desirable sludge dewatering

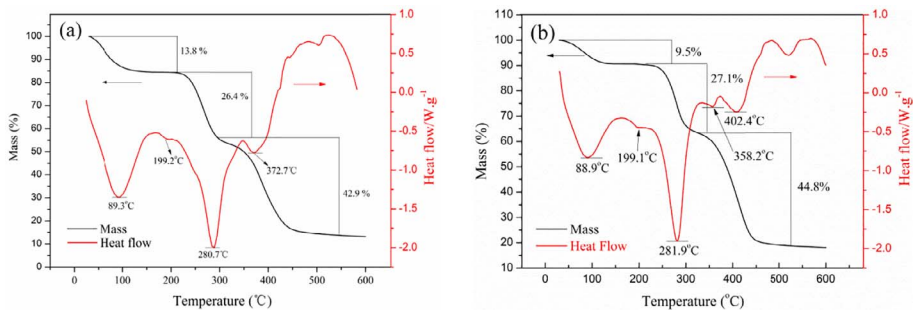


Fig. 7. Thermogravimetric curves of (a) CPADM and (b) TPADM.

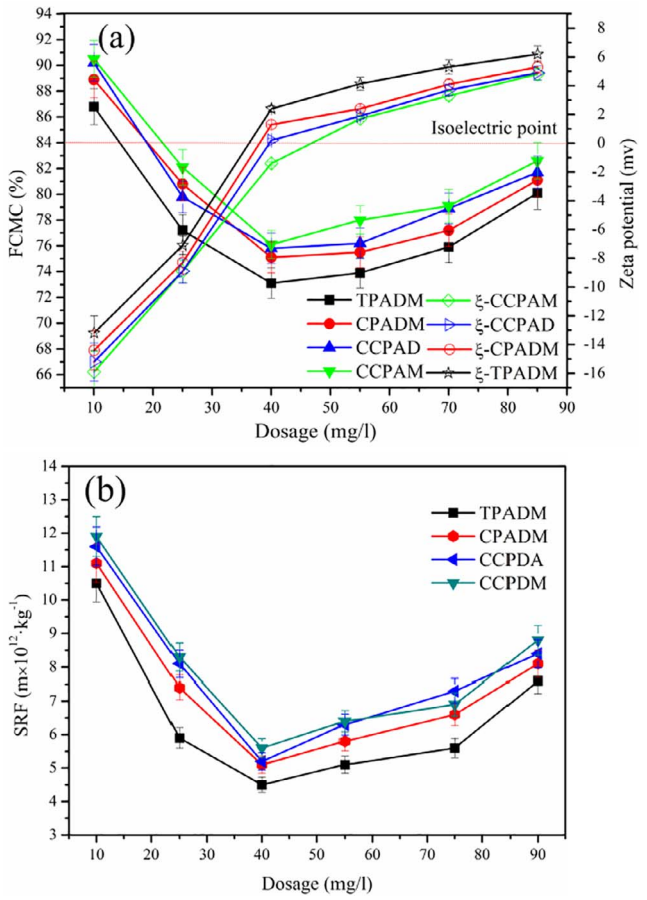


Fig. 8. Effect of dosage on (a) FCMC and zeta potential, and (b) SRF.

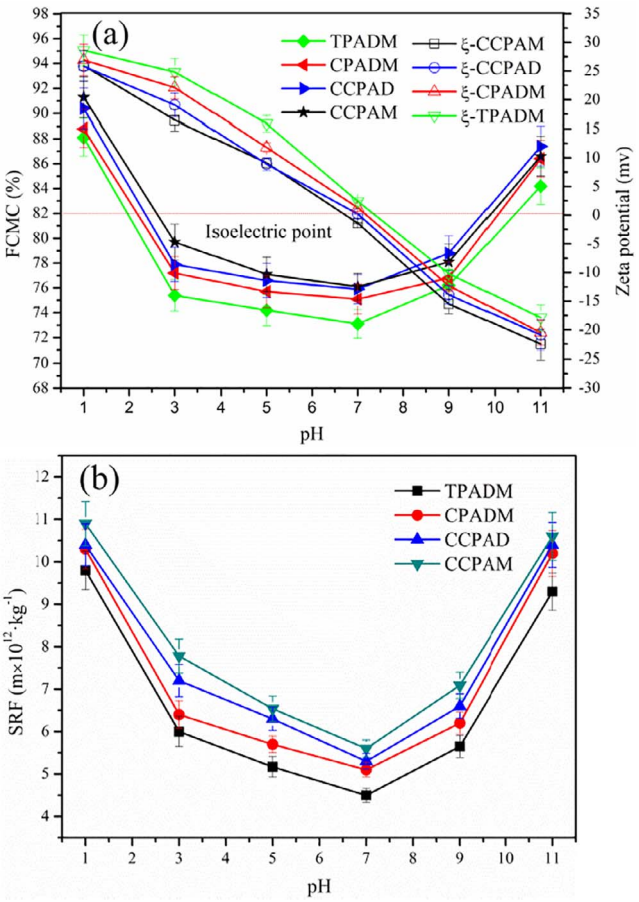


Fig. 9. Effect of the pH on the (a) FCMC and zeta potential, and (b) SRF.

performance at a pH scope of 5–9, which indicated that this novel flocculant had an excellent acid and alkali endurance, thus broadening the scope of pH application.

3.5. Floc properties

The sludge floc size and the fractal dimension (D_f) have been widely used to evaluate the flocculation performance and sludge dewatering ability of the flocculants [40]. Larger and compacter floc is more conducive to dewatering, while small floc can easily plug the filter holes and increase specific filtration resistance, thus deteriorating the dewatering performance [28,41]. Therefore, it is significant to investigate the sludge floc size and the fractal dimension (D_f).

Fig. 10 showed the variations in fractal dimension (D_f) as a function of flocculants dosage. It was clear that the flocculants (TPADM, CPADM, CCPAD and CCPAM) showed a different D_f between 1.271 and 1.490, even though their molecular weight and cationic degree were the same. This phenomenon was supposed to connect with their bridging and charge neutralization ability. Long-chain polymers adsorbed on particles can have loops and tails extending some way into solution. This gives the possibility of attachment of these dangling polymer segments to other particles, thus bridging particles together to form the original floc structure. However, due to the repulsive force between the negatively charged particles, the yielded flocs under bridging always failed in constructing a more compact and dense floc structure. Moreover, TPADM with the cationic microblock had the highest D_f among the cationic flocculants, which indicated that the cationic microblock contributed to much to the D_f. Because the cationic microblock could significantly increase the TPADM charge neutralization ability, and once the TPADM was added to the sludge samples, the negatively charged particles would be attracted and neutralized completely, and

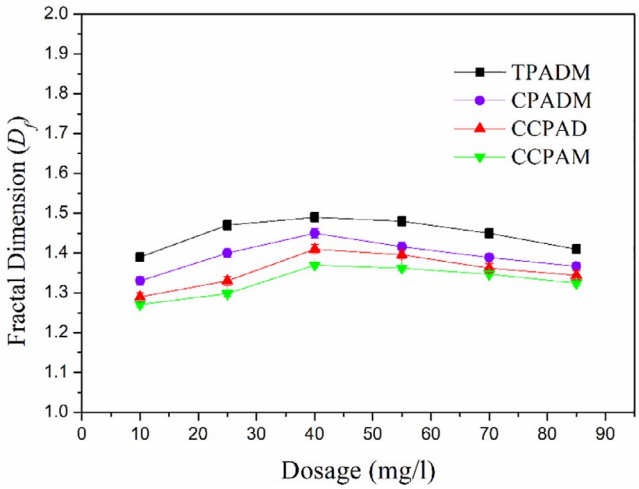


Fig. 10. The sludge floc fractal dimension (D_f) for different flocculants.

then combined with the polymer chain tightly to form compact and dense flocs structure [42,43]. Therefore, the D_f was raised and the sludge dewatering efficiency was further enhanced.

Fig. 11 illustrated the floc size distribution after adding TPADM, CPADM, CCPAD and CCPAM at the optimal dosage of 40 $mg \cdot L^{-1}$ and pH of 7.0. The floc size of TPADM was larger than the others, and the difference of their floc size distribution was evident. Compared with CPADM, CCPAD and CCPAM, the flocs size characterized with the median equivalent volumetric diameter (d_{50}) was the largest for TPADM (439.156 μm). The cationic microblocks resulted in a large flocs

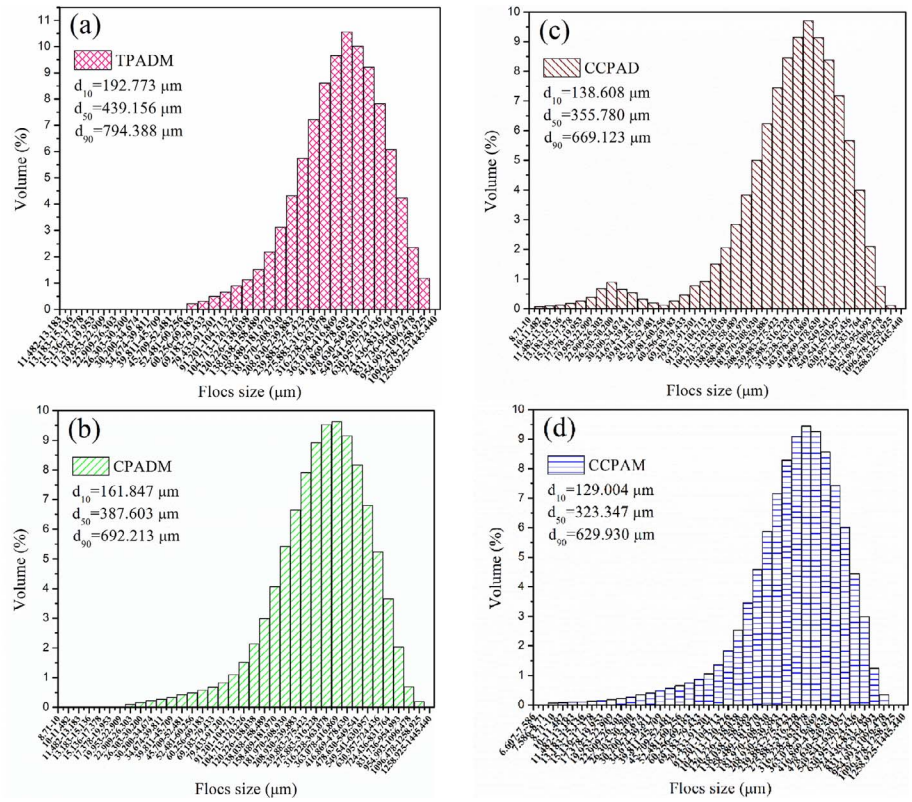


Fig. 11. Sludge flocs size distribution for (a) TPADM, (b) CPADM, (c) CCPAD and (d) CCPAM.

size. The TPADM with blocky distributed cationic groups had a stronger charge neutralization capacity, whereas the flocculants with randomly distributed cationic units did not. Therefore, more particles were tightly absorbed on the polymer chain to form a larger and compact flocs. Meanwhile, the repulsion between charged segments could induce the chain expansion and embedding into the sludge solution, thereby leading to a significant bridging effect. In this condition, the number of particles adsorbed by the cationic microblock structure was more than the number adsorbed by the random distributed cationic monomers, which was beneficial for the large and dense flos formation.

4. Flocculation mechanism

Based on the analytical results of zeta potential, SRF, FCMC, floc size and D_f, the possible flocculation mechanism involved in the flocculation process was summarized and displayed in Fig. 12. Because of the formation of the cationic microblocks in TPADM, the charge density and intensity was extremely increased, thereby greatly improving the charge neutralization ability of the TPADM. Besides, the cationic microblock would generate a strong electrical repulsion, which was favorable for the stretch and extension of TPADM polymer chain. As a result, the bridging effect of the TPADM was increased. The negatively charged sludge particles were neutralized completely and aggregated to form large and compact flocs under the charge neutralization and bridging. These larger and compact flocs acted as a stable skeleton construction and could withstand high pressure test, and hence more and more stable channels and voids formed [44,45]. Therefore, it was easy for the water moisture to pass though the stable channels and voids and the sludge filtration resistance and moisture content reached the minimum.

5. Conclusions

To enhance and improve the active sludge dewatering, a new

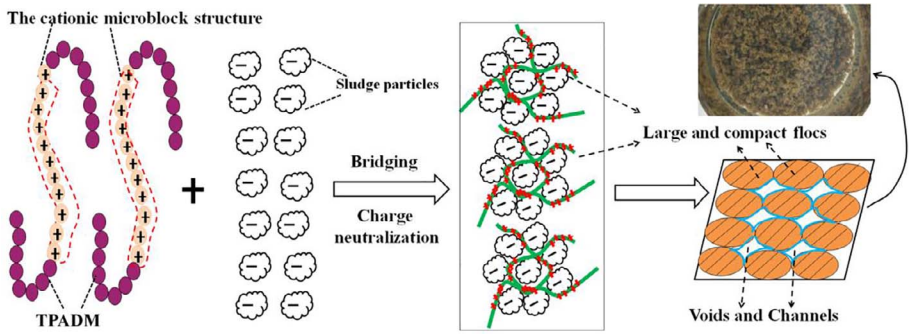


Fig. 12. Possible flocculation mechanism of the TPADM.

cationic flocculant TPADM with the microblock structure was successfully synthesized by polymerization of AM, DMDAAC and NaPAA via US-initiated template copolymerization. According to the instrumental analysis results of FT-IR, ^{1}H NMR and TGA, it was conformed that the novel cationic microblock structure was successfully synthesis through the US-initiated template copolymerization. Moreover, a high K_M value of 12.85 between NaPAA and DMDAAC reflected I (zip) template polymerization mechanism and also the microblock structure formation. The factors that affected the polymerization were discussed and the optimal reaction factors were exhibited at ultrasonic power of 150 W, ultrasonic time of 20 min, 30.0 wt% monomer concentration, 0.06 wt‰ of initiator concentration, m_{AM}:m_{DMDAAC} of 3:1 and n_{NaPAA}:n_{DMDAAC} of 1:1. The sludge dewatering test indicated that the microblock structure in TPADM could extremely enhance the flocculant charge neutralization and bridging ability, thus contributing much to the formation of floc with a large size (d_{50}:439.156 μm) and compact structure (D_f:1.490). In this condition, these larger and compact flocs acted as a stable and pressure proof skeleton structure, which was favorable for the formation of stable channels and voids. As a result, a superior sludge dewatering performance (FCMC: 73.1% and SRF: 4.5×10^{12} m·kg^{-1}) were acquired at pH of 7.0, dosage of 40 mg·L^{-1}.

Conflict of interest

The authors declare that they have no conflict of interest.

Acknowledgements

The authors are grateful for the financial support provided by the National Natural Science Foundation of China (Project No. 21677020 and 21477010).

Appendix A. Supplementary data

Supplementary data associated with this article can be found, in the online version, at http://dx.doi.org/10.1016/j.ultsonch.2018.02.017.

References

[1] C.X. Li, X.D. Wang, G.Y. Zhang, G.W. Yu, J.J. Lin, Y. Wang, Hydrothermal and alkaline hydrothermal pretreatments plus anaerobic digestion of sewage sludge for dewatering and biogas production: bench-scale research and pilot-scale verification, Water Res. 117 (2017) 49–57.
[2] L.L. Qian, S.Z. Wang, D.H. Xu, Y. Guo, X.Y. Tang, L.S. Wang, Treatment of municipal sewage sludge in supercritical water: a review, Water Res. 89 (2016) 118–131.
[3] T.T. More, S. Yan, R.D. Tyagi, R.Y. Surampalli, Potential use of filamentous fungi for wastewater sludge treatment, Bioresour. Technol. 101 (2010) 7691–7700.
[4] X.H. Zhang, H.Y. Lei, K. Chen, Z. Liu, H. Wu, H.Y. Liang, Effect of potassium ferrate (K_2FeO_4) on sludge dewaterability under different pH conditions, Chem. Eng. J. 210 (2012) 467–474.
[5] T.T. More, S. Yan, R.P. John, R.D. Tyagi, R.Y. Surampalli, Biochemical diversity of the bacterial strains and their biopolymer producing capabilities in wastewater sludge, Bioresour. Technol. 121 (2012) 304–311.
[6] S.J. Skinner, L.J. Studer, D.R. Dixon, P. Hillis, C.A. Rees, R.C. Wall, R.G. Cavalida, S.P. Usher, A.D. Stickland, P.J. Scales, Quantification of wastewater sludge dewatering, Water Res. 82 (2015) 2–13.
[7] Y. Liao, H.L. Zheng, L. Qian, Y.J. Sun, L. Dai, W.W. Xue, UV-initiated polymerization of hydrophobically associating cationic polyacrylamide modified by a surface-active monomer: a comparative study of synthesis, characterization, and sludge dewatering performance, Ind. Eng. Chem. Res. 53 (2014) 11193–11203.
[8] H.L. Zheng, Y.J. Sun, C.J. Zhu, J.S. Guo, C. Zhao, Y. Liao, Q.Q. Guan, UV-initiated polymerization of hydrophobically associating cationic flocculants: synthesis, characterization, and dewatering properties, Chem. Eng. J. 234 (2013) 318–326.
[9] H. Liimatainen, J. Sirviö, O. Sundman, M. Visanko, O. Hormi, J. Niinimäki, Flocculation performance of a cationic biopolymer derived from a cellulosic source in mild aqueous solution, Bioresour. Technol. 102 (2011) 9626–9632.
[10] M.G. Rasteiro, I. Pinheiro, H. Ahmadloo, D. Hunkeler, F.A.P. Garcia, P. Ferreira, C. Wandrey, Correlation between flocculation and adsorption of cationic polyacrylamides on precipitated calcium carbonate, Chem. Eng. Res. Des. 95 (2015) 298–306.
[11] Y.X. Zhang, F.P. Wu, M.Z. Li, E.J. Wang, Novel approach to synthesizing hydrophobically associating copolymer using template copolymerization: the synthesis and behaviors of acrylamide and 4-(ω-propenoyloxyethoxy) benzoic acid copolymer, J. Phys. Chem. B 109 (2005) 22250–22255.
[12] J.H. Li, Y.S. Li, Y.N. Song, S. Niu, N. Li, Ultrasonic-assisted synthesis of polyvinyl alcohol/phytic acid polymer film and its thermal stability, mechanical properties and surface resistivity, Ultrason. Sonochem. 39 (2017) 853–862.
[13] C. Zhu, P.Y. Zhang, H.J. Wang, J. Ye, Conditioning of sewage sludge via combined ultrasonication-flocculation-skeleton building to improve sludge dewaterability, Ultrason. Sonochem. 40 (2018) 353–360.
[14] M.J.S. Fard, P. Hayati, A. Firoozadeh, J. Janczak, Ultrasonic synthesis of two new zinc(II) bipyridine coordination polymers: new precursors for preparation of zinc (II) oxide nano-particles, Ultrason. Sonochem. 35 (2017) 502–513.
[15] Y.J. Sun, C.Y. Zhu, W.Q. Sun, Y.H. Xu, X.F. Xiao, H.L. Zheng, H.F. Wu, C.Y. Liu, Plasma-initiated polymerization of chitosan-based CS-g-P(AM-DMDAAC) flocculant for the enhanced flocculation of low-algal-turbidity water, Carbohy. Polym. 164 (2017) 222–232.
[16] J.Y. Ma, K. Fu, J. Shi, Y.J. Sun, X.X. Zhang, L. Ding, Ultraviolet-assisted synthesis of polyacrylamide-grafted chitosan nanoparticles and flocculation performance, Carbohy. Polym. 151 (2016) 565–575.
[17] P.S. Nrianjan, K.T. Amit, K.U.J. Santosh, Polymerization of acrylamide in a micellar medium: inhibition effect of surfactants, J. Appl. Polym. Sci. 122 (2011) 981–986.
[18] H.Z. Shang, J.P. Liu, Y.B. Zheng, L.G. Wang, Synthesis, characterization, and flocculation properties of poly(acrylamide-methacryloxyethyltrimethyl ammonium chloride methacryloxypropyltrimethoxy silane), J. Appl. Polym. Sci. 111 (2009) 1594–1599.
[19] H.J. Ren, W. Chen, Y.F. Zheng, Z.K. Luan, Effect of hydrophobic group on flocculation properties and dewatering efficiency of cationic acrylamide copolymers, React. Funct. Polym 67 (2007) 601–608.
[20] S. Połowiński, Template polymerisation and co-polymerisation, Prog. Polym. Sci. 27 (2002) 537–577.
[21] X.M. Wang, M.H. Li, X.J. Song, Z.H. Chen, B.D. Wu, S.J. Zhang, Preparation and evaluation of titanium-based xerogel as a promising coagulant for water/wastewater treatment, Environ. Sci. Technol. 50 (2016) 9619–9626.
[22] B.A. Bhanvase, D.V. Pinjari, S.H. Sonawane, P.R. Gogate, A.B. Pandit, Analysis of semibatch emulsion polymerization: role of ultrasound and initiator, Ultrason. Sonochem. 19 (2012) 97–103.
[23] X.Q. Cui, A.L. Rosa, Investigation of the probe-sample interaction in the ultrasonic/shear-force microscope: the phononic friction mechanism, Appl. Phys. Lett. 87 (2005) 231907.
[24] J.Y. Ma, J. Shi, H.C. Ding, G.C. Zhu, K. Fu, X. Fu, Synthesis of cationic polyacrylamide by low-pressure UV initiation for turbidity water flocculation, Chem. Eng. J. 312 (2017) 20–29.
[25] X. Li, H.L. Zheng, B.Y. Gao, C. Zhao, Y.J. Sun, UV-initiated polymerization of acid- and alkali-resistant cationic flocculant P(AM-MAPTAC): synthesis, characterization, and application in sludge dewatering, Sep. Puri. Technol. 187 (2017) 244–254.
[26] X.H. Peng, X.C. Peng, Water-soluble copolymers. II. Inverse emulsion terpolymerization of acrylamide, sodium acrylate, and acryloyloxyethyl trimethylammonium chloride, J. Appl. Polym. Sci. 101 (2006) 1381–1385.
[27] J.R. Zhu, H.L. Zheng, Z.Z. Jiang, Z. Zhang, L.W. Liu, Y.J. Sun, T. Tshukudu, Synthesis and characterization of a dewatering reagent: cationic polyacrylamide (P(AM-DMC-DAC)) for activated sludge dewatering treatment, Desalin. Water Treat. 51 (2013) 2791–2801.
[28] W. Chen, H.L. Zheng, Q.Q. Guan, H.K. Teng, C.L. Zhao, C. Zhao, Fabricating a flocculant with controllable cationic microblock structure: characterization and sludge conditioning behavior evaluation, Ind. Eng. Chem. Res. 55 (2016) 2892–2902.
[29] X. Li, H.L. Zheng, B.Y. Gao, Y.J. Sun, B.Z. Liu, C.L. Zhao, UV-initiated template copolymerization of AM and MAPTAC: microblock structure, copolymerization mechanism, and flocculation performance, Chemosphere 167 (2017) 71–81.
[30] H.X. Chen, H.M. Tang, X.Y. Wu, Y.G. Liu, J.H. Bai, F. Zhao, Synthesis, characterization, and property evaluation of a hydrophobically modified polyacrylamide as enhanced oil recovery chemical, J. Dispersion Sci. Technol. 37 (2016) 486–495.
[31] X.J. Yang, L. Ni, Synthesis of hybrid hydrogel of poly(AM co DADMAC)/silica sol and removal of methyl orange from aqueous solutions, Chem. Eng. J. 209 (2012) 194–200.
[32] X.M. Zhang, G.C. Jiang, Y. Xuan, L. Wang, X.B. Huang, Associating copolymer acrylamide/diallyldimethylammonium chloride/butyl acrylate/2-acrylamido-2-methylpropanesulfonic acid as a tackifier in clay-free and water-based drilling fluids, Energy Fuels 31 (2017) 4655–4662.
[33] Z. Abdollahi, M. Frounchi, S. Dadbin, Synthesis, characterization and comparison of PAM, cationic PDMC and P(AM-co-DMC) based on solution polymerization, J. Ind. Eng. Chem. 17 (2011) 580–586.
[34] C.Y. Ou, C.H. Zhang, S.D. Li, L. Yang, J.J. Dong, X.L. Mo, M.T. Zeng, Thermal degradation kinetics of chitosan-cobalt complex as studied by thermogravimetric analysis, Carbohy. Polym. 82 (2010) 1284–1289.
[35] H.L. Zheng, L. Feng, B.Y. Gao, Y.H. Zhou, S.X. Zhang, B.C. Xu, Effect of the cationic block structure on the characteristics of sludge flocs formed by charge neutralization and patching, Materials 10 (2017) 487.
[36] Z. Yang, H. Yang, Z.W. Jiang, T. Cai, H.J. Li, H.B. Li, A. Li, R.S. Cheng, Flocculation of both anionic and cationic dyes in aqueous solutions by the amphoteric grafting flocculant carboxymethyl chitosan-graft-polyacrylamide, J. Hazard. Mater. 255

(2013) 36–45.
[37] L.H. Lu, Z.D. Pan, N. Hao, W.Q. Peng, A novel acrylamide-free flocculant and its application for sludge dewatering, Water Res. 57 (2014) 304–312.
[38] K.E. Lee, N. Morad, B.T. Poh, T.T. Teng, Comparative study on the effectiveness of hydrophobically modified cationic polyacrylamide groups in the flocculation of kaolin, Desalination 270 (2011) 206–213.
[39] D.F. Wang, T.Q. Zhao, L.Q. Yan, Z.M. Mi, Q. Gu, Y.M. Zhang, Synthesis, characterization and evaluation of dewatering properties of chitosan-grafting DMDAAC flocculants, Int. J. Biol. Macromol. 92 (2016) 761–768.
[40] Y.X. Zhao, B.Y. Gao, Q.B. Qi, Y. Wang, S. Phuntsho, J.H. Kim, Q.Y. Yue, Q. Li, H.K. Shon, Cationic polyacrylamide as coagulant aid with titanium tetrachloride for low molecule organic matter removal, J. Hazard. Mater. 259 (2013) 84–92.
[41] L. Fabrizi, B. Jefferson, S.A. Parsons, A. Wetherill, P. Jarvis, The role of polymer in improving floc strength for filtration, Environ. Sci. Technol. 44 (2010) 6443–6449.
[42] P.T. Zhao, S.F. Ge, Z.Q. Chen, X. Li, Study on pore characteristics of flocs and sludge dewaterability based on fractal methods (pore characteristics of flocs and sludge dewatering), Appl. Therm. Eng. 58 (2013) 217–223.
[43] Z.B. Wang, J. Nan, M. Yao, Y.M. Yang, Effect of additional polyaluminum chloride and polyacrylamide on the evolution of floc characteristics during floc breakage and re-growth process, Sep. Puri. Technol. 173 (2017) 144–150.
[44] H.J. Luo, X.A. Ning, X.J. Liang, Y.F. Feng, J.Y. Liu, Effects of sawdust-CPAM on textile dyeing sludge dewaterability and filter cake properties, Bioresour. Technol. 139 (2013) 330–336.
[45] W.S. Chen, F.C. Chang, Y.H. Shen, M.S. Tsai, The characteristics of organic sludge/sawdust derived fuel, Bioresour. Technol. 102 (2011) 5406–5410.